THE JOURNAL OF BIOLOGICAL CHEMISTRY
Vol. 277, No. 12, Issue of March 22, pp. 10121–10128, 2002

Printed in U.S.A.

Architecture of the p40-p47-p67^{phox} Complex in the Resting State of the NADPH Oxidase

A CENTRAL ROLE FOR p67^{phox}*

Received for publication, December 18, 2001, and in revised form, January 15, 2002
Published, JBC Papers in Press, February 16, 2002, DOI 10.1074/jbc.M112065200

Karine Lapouge, Susan J. M. Smith, Yvonne Groemping, and Katrin Rittinger‡

From the Division of Protein Structure, National Institute for Medical Research, Mill Hill, London NW7 1AA, United Kingdom

The phagocyte NADPH oxidase is a multiprotein enzyme whose subunits are partitioned between the cytosol and plasma membrane in resting cells. Upon exposure to appropriate stimuli multiple phosphorylation events in the cytosolic components take place, which induce rearrangements in a number of protein-protein interactions, ultimately leading to translocation of the cytoplasmic complex to the membrane. To understand the molecular mechanisms that underlie the assembly and activation process we have carried out a detailed study of the protein-protein interactions that occur in the p40-p47-p67^{phox} complex of the resting oxidase. Here we show that this complex contains one copy of each protein, which assembles to form a heterotrimeric complex. The apparent high molecular weight of this complex, as observed by gel filtration studies, is due to an extended, non-globular shape rather than to the presence of multiple copies of any of the proteins. Isothermal titration calorimetry measurements of the interactions between the individual components of this complex demonstrate that p67^{phox} is the primary binding partner of p47^{phox} in the resting state. These findings, in combination with earlier reports, allow us to propose a model for the architecture of the resting complex in which p67^{phox} acts as the bridging molecule that connects p40^{phox} and p47^{phox}.

The phagocytic NADPH oxidase is a multiprotein enzyme that catalyzes the reduction of molecular oxygen to superoxide in response to invasion of the body with bacterial, fungal, and viral pathogens. Superoxide anions are precursors of a variety of reactive oxygen species that are used for killing of the microorganisms (reviewed in Refs. 1–4). The importance of the NADPH oxidase in host defense is exemplified by the inherited disorder chronic granulomatous disease in which patients suffer from recurring infections due to a defect in oxidase activity. The NADPH oxidase consists of six subunits. Four of these, p40^{phox}, p47^{phox}, p67^{phox},[1] and the small GTPase Rac are cytosolic in unstimulated cells, whereas p22^{phox} and gp91^{phox} form a heterodimeric, membrane-bound flavocytochrome, also known as cytochrome b_{558}. In resting cells, p40^{phox}, p47^{phox}, and p67^{phox} exist as a tight cytosolic complex of undefined stoichiometry that can be purified by gel filtration chromatography with an apparent molecular mass of 250–300 kDa (5–8). Activation of the NADPH oxidase is initiated by phosphorylation, which is believed to induce conformational changes that subsequently lead to rearrangements in intra- and intermolecular interactions in the p40-p47-p67^{phox} complex (9–14). These events culminate in translocation of this complex to the membrane and association with both Rac-GTP and cytochrome b_{558} to form the active enzyme.

p40^{phox}, p47^{phox}, and p67^{phox} are multidomain proteins that contain SH3 protein-protein interaction domains (see Fig. 1). Additionally, p40^{phox} and p47^{phox} each contain a PX domain, which has recently been shown to bind to phosphatidylinositols and seems to act as a membrane-targeting module (15–18). Most PX domains identified so far also contain a Pro-*X*-*X*-Pro motif, which is the consensus target sequence for SH3 domain binding modules (19). This suggests that PX domains are bifunctional with the potential to coordinate membrane localization as well as protein assembly during signal transduction events. In support of this idea, it has been shown that the isolated PX domain of p47^{phox} binds to the second SH3 domain of p47^{phox} with an equilibrium dissociation constant (K_d) of ~50 μM (20).

p47^{phox} plays a central role in the activation process due to its ability to bind to the cytoplasmic region of p22^{phox}, an interaction that is necessary for oxidase activity (21–23). p47^{phox} contains a PX domain, tandem SH3 domains, and a polybasic region followed by a proline-rich sequence within its C-terminal region (Fig. 1). Studies by various groups suggest that p47^{phox} exists in an autoinhibited conformation in the resting state. In this model, the tandem SH3 domains are masked due to an intramolecular interaction with a C-terminal segment whereas the P*XX*P motif present in the PX domain simultaneously interacts with the second SH3 domain (24, 25). *In vivo* phosphorylation of multiple serine residues within the C terminus of p47^{phox} liberates the N-terminal SH3 domain and allows it to interact with a proline-rich region in p22^{phox}. This, in turn, initiates translocation of the cytoplasmic complex to the membrane and activation of the oxidase (10, 12, 21, 24–28).

p67^{phox} is complexed with p47^{phox} in the cytosol of resting neutrophils, and this interaction is absolutely required for translocation of p67^{phox} to the membrane. Evidence for this is provided by the observation that neither p67^{phox} nor p40^{phox} are able to translocate in chronic granulomatous disease neutrophils lacking p47^{phox} (29–31). Once at the membrane, p67^{phox} interacts with Rac and possibly cytochrome b_{558} to support catalysis by a mechanism that is not fully understood (32–37). On the other hand, no clear function has yet been

* The costs of publication of this article were defrayed in part by the payment of page charges. This article must therefore be hereby marked "*advertisement*" in accordance with 18 U.S.C. Section 1734 solely to indicate this fact.

‡ To whom correspondence should be addressed. Tel.: 44-20-8959-3666; Fax: 44-20-8913-8569; E-mail: katrin.rittinger@nimr.mrc.ac.uk.

[1] The abbreviations used are: phox, phagocyte oxidase; ITC, isothermal titration calorimetry; SH3, Src homology 3; PX, PhoX domain; TPR, tetratricopeptide repeat; DLS, dynamic light scattering; GST, glutathione *S*-transferase; Ni-NTA, nickel-nitrilotriacetic acid.

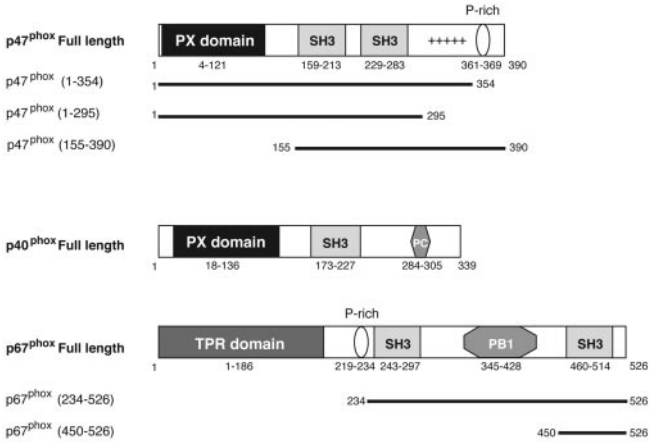

FIG. 1. **Schematic showing the domain structure of the cytosolic components of the NADPH oxidase.** The borders of the individual domains have been taken from the Pfam and the Prosite data bases. Shown are the sizes of the full-length and truncated proteins used in this study.

attributed to p40^{phox}, and it can apparently act as an activator or inhibitor depending on the experimental system. Furthermore, there are suggestions that it might stabilize p67^{phox} and thus act as a general modulator of NADPH oxidase activity (38–40).

Extensive efforts have been made to identify domains involved in the multiple protein-protein interactions and conformational changes that take place during NADPH oxidase activation. Nevertheless, the precise nature of the protein-protein interactions that occur during the different stages of the activation process and how these are affected by phosphorylation are still a matter of debate. In particular the C-terminal proline-rich region in p47^{phox} has been variously suggested to bind to SH3 domains present in p67^{phox} and p40^{phox}, as well as to the tandem SH3 domains present within p47^{phox} itself (21–23, 25, 41–45). Furthermore, there are conflicting reports concerning the architecture of the p40-p47-p67^{phox} complex in resting cells. In one scenario, p40^{phox} acts as an adaptor that holds p47^{phox} and p67^{phox} together whereas an alternative model assumes that p67^{phox} acts as a bridging molecule between p40^{phox} and p47^{phox} (1, 29, 39, 41, 44, 46, 47). A likely explanation for the detection of multiple binding partners for a particular region is that many previous studies have made use of isolated domains. It is possible that such an approach may exclude additional regions that contribute to specificity and/or affinity. In addition, many of the techniques used do not allow a precise quantitative assessment of the affinity of any particular interaction. For these reasons, the relative significance of one interaction with respect to another becomes difficult to assess. Nevertheless, it is possible that all interactions detected so far do take place at various stages of the activation process but occur in a sequential not a simultaneous manner.

Here we describe the thermodynamic and hydrodynamic characterization of protein-protein complexes of the cytosolic components of the NADPH oxidase. Using a combination of isothermal titration calorimetry, analytical ultracentrifugation, and gel filtration chromatography we demonstrate that p40^{phox}, p47^{phox}, and p67^{phox} form a trimeric protein complex with a 1:1:1 stoichiometry. Furthermore, we show unequivocally that p67^{phox} is the adaptor that links p40^{phox} and p47^{phox} in the resting complex, providing a solid framework upon which the activation process can be further investigated.

EXPERIMENTAL PROCEDURES

Protein Purification—The DNA sequences encoding full-length p67^{phox} (1–526), p67^{phox} (234–526), and p67^{phox} (450–526) "p67-SH3$_B$" were cloned into pGEX-4T1 (Amersham Biosciences, Inc.) and fusion proteins were overexpressed in *Escherichia coli* BL21. The cells were lysed in a buffer containing 50 mM Tris-HCl, pH 7.5, 300 mM NaCl, 2 mM EDTA, 4 mM dithiothreitol, 4 mM benzamidine, and 1 mM phenylmethylsulfonyl fluoride, and the protein was purified on glutathione-Sepharose 4B beads (Amersham Biosciences, Inc.). The GST-tag was removed using human thrombin (Calbiochem). Further purification was carried out on a Source Q anion-exchange column (Amersham Biosciences, Inc.) equilibrated in 50 mM Tris-HCl, pH 7.5, 50 mM NaCl, 1 mM EDTA, and 4 mM dithiothreitol. Proteins were eluted with a 50 mM to 1 M NaCl gradient in the same buffer. Fractions containing pure protein were pooled and concentrated by ultrafiltration to around 20 mg/ml.

DNA sequences encoding full-length p47^{phox} (1–390), p47^{phox} (1–295), p47^{phox} (1–354), and p47^{phox} (155–390) were cloned into pGEX-6P1, and fusion proteins were overexpressed in *E. coli* BL21. Cells were lysed in 50 mM Tris-HCl, pH 7.0, 300 mM NaCl, 2 mM EDTA, 4 mM dithiothreitol, 4 mM benzamidine, and 1 mM phenylmethylsulfonyl fluoride. The protein was purified on glutathione-Sepharose 4B beads, and the GST-tag was removed by incubation with PreScission Protease (Amersham Biosciences, Inc.). Further purification was carried out on a Source S column equilibrated in 50 mM HEPES, pH 8.0, 50 mM NaCl, 1 mM EDTA, and 2 mM dithiothreitol, and proteins were eluted with a 50 mM to 500 mM NaCl gradient in the same buffer. Fractions containing pure protein were pooled and concentrated by ultrafiltration to around 50 mg/ml.

p40^{phox} cloned into pET-23d (Novagen) was a kind gift of Frans Wientjes, University College, London. The protein was overexpressed in *E. coli* BL21(DE3) and purified on Ni-NTA beads (Qiagen) equilibrated with 50 mM NaH_2PO_4, pH 8.0, 300 mM NaCl, 5 mM mercaptoethanol, and 20 mM imidazole. p40^{phox} was eluted with a 20 mM to 1 M imidazole gradient. Fractions containing pure protein were pooled, dialyzed against 2 liters of 50 mM HEPES, pH 8.0, 50 mM NaCl, and 2 mM DTT, and concentrated by ultrafiltration to ~10 mg/ml.

All sequences were confirmed by nucleotide sequencing and electrospray mass spectrometry of the purified proteins. Protein concentrations were determined spectroscopically using calculated absorption coefficients.

Complexes of p67-p40^{phox}, p67-p47^{phox}, and p67-p47-p40^{phox} were obtained by mixing the proteins in 1:1 stoichiometries and purification by gel filtration on a Superdex 200 column (Amersham Biosciences, Inc.) using a buffer containing 50 mM HEPES, pH 7.0, 100 mM NaCl, and 2 mM DTT for p47-p67^{phox} and p40-p47-p67^{phox} and pH 8.0 for p40-p67^{phox}. Fractions containing the complexes were concentrated by ultrafiltration to ~10 mg/ml.

Dynamic Light Scattering—Dynamic light scattering (DLS) measurements were performed on a DynaPro-801 dynamic light-scattering instrument (Protein Solution). Samples were filtered through 0.02-μm filters, and experiments were performed at sample concentrations of 0.5 to 2 mg/ml in the same buffer used for analytical ultracentrifugation measurements. Data were analyzed by autocorrelation, and the resulting autocorrelation function was then evaluated using single-exponential cumulant analysis. From this the translational diffusion coefficient was determined, which can subsequently be used to derive the hydrodynamic radius and thereby the molecular weight using an empirically derived relationship between the radius and molecular weights for globular proteins. All calculations were carried out using the software package supplied with the machine.

Analytical Ultracentrifugation—The protein partial-specific volume, solvent density, and viscosity were calculated using the SEDNTERP program (John Philo). Sedimentation equilibrium and velocity studies were carried out using a Beckman Optima XLA analytical ultracentrifuge. Prior to centrifugation protein samples were dialyzed exhaustively against a buffer containing 50 mM HEPES, 100 mM NaCl, 1 mM EDTA, and 2 mM β-mercaptoethanol adjusted to the pH used for purification. Equilibrium experiments were carried out on 110-μl samples in an An-60ti rotor using six-channel centerpieces with protein absorbances of 0.8 OD, 0.5 OD, and 0.3 OD at λ = 280 nm and three different rotor speeds (p67^{phox} at 12,000, 15,000, and 18,000 rpm; p40^{phox} and p47^{phox} at 10,000, 13,000, and 18,000 rpm; p40-p47^{phox}, p40-p67^{phox}, and p47-p67^{phox} at 7000, 8500, and 12,500 rpm; p40-p47-p67^{phox} at 6000, 8000, and 11,000 rpm). Radial scans of the absorbance at 280 nm (path length 1.2 cm) were measured at 0.001-cm intervals, at 15 °C and 20-fold averaged. Scans indicating that equilibrium had been reached were used for analysis (typically around 20 h). Multiple data sets were analyzed by non-linear least-squares procedures provided in the Beckman Optima XL-A/XL-1 data analysis software, version 4.1.

Sedimentation velocity studies were carried out at protein concen-

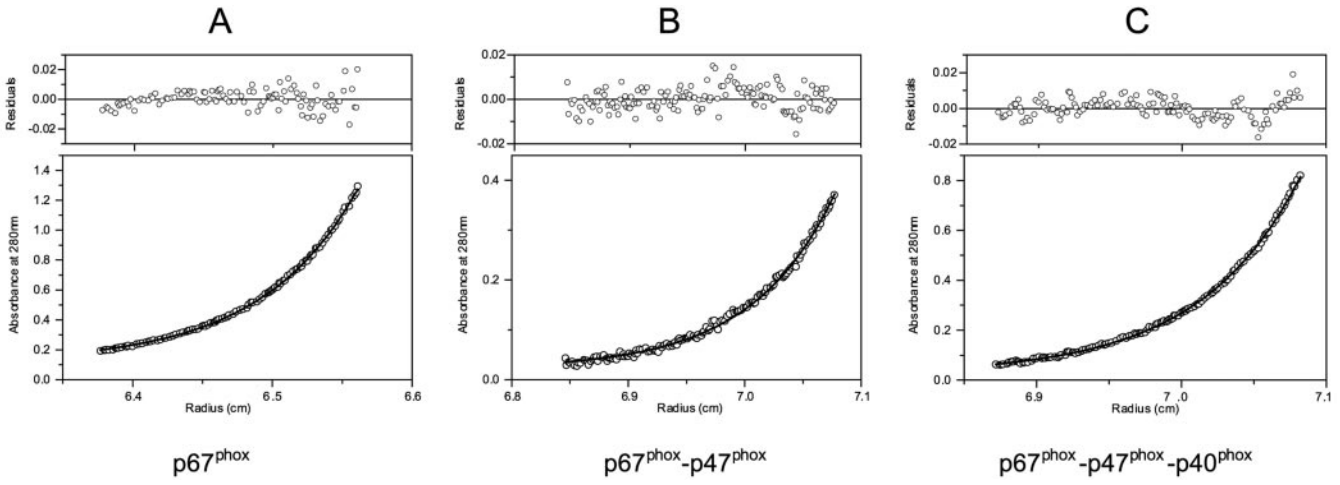

FIG. 2. **Determination of solution molecular masses by sedimentation equilibrium.** The *lower panels* show the equilibrium data and the best fits (*continuous curves*). The *upper panel* shows the residuals plotted *versus* radial position. *A*, equilibrium distribution of p67^{phox} at a loading concentration of 7.5 μM, rotor speed 18,000 rpm, 15 °C. *B*, equilibrium distribution of p47-p67^{phox} at a loading concentration of 2.4 μM, rotor speed 12,500 rpm, 15 °C. *C*, equilibrium distribution of p40-p47-p67^{phox} at a loading concentration of 1.8 μM, rotor speed 11,000 rpm, 15 °C.

trations between 0.2 and 1 mg/ml and sedimentation boundaries were monitored at λ = 280 nm. The data were analyzed using the program SVEDBERG, which directly fits sedimentation velocity profiles to give the sedimentation (s) and diffusion coefficient (D) (48). Values obtained in this way were then extrapolated to zero concentration and corrected to standard conditions to yield $s_{20,w}$ and $D_{20,w}$. Hydrodynamic shape parameters, including frictional (f/f_0) and axial ratios (a/b) were calculated with the program SEDNTERP using the v-bar method.

Isothermal Titration Calorimetry—Isothermal calorimetric titrations were performed with a Microcal omega VP-ITC (MicroCal Inc., Northampton, MA). All proteins were dialyzed against ITC buffer (25 mM HEPES, 50 mM NaCl, 1 mM EDTA, 2 mM DTT; at the same pH used for purification), and experiments were performed at 15 °C. Typically solutions of 10–20 μM of proteins or complexes in the cell were titrated by injection of a total of 290 μl of 100–200 μM of ligands (49). Heats of dilution of ligand into buffer were determined in control experiments and subtracted from the raw data of the binding experiment prior to data analysis. Data were fitted by least-squares procedures using the evaluation software, Microcal Origin version 5.0 provided by the manufacturer. The data were averaged over two to five ITC experiments. Titrations that followed a two-site binding isotherm were additionally carried out in the presence of 2 mM tris-(2-carboxyl)phosphine to ensure that the second binding site detected was not an artifact caused by the use of DTT.

Analytical Gel Filtration—Analytical gel filtration chromatography was carried out on a Superdex 200 HR 10/30 column (Amersham Biosciences, Inc.) equilibrated with 50 mM HEPES, pH 7.0, 100 mM NaCl, and 2 mM $MgCl_2$ at a flow rate of 0.4 ml/min.

RESULTS

Analytical Ultracentrifugation Studies

The proteins used in this study have been overexpressed in *E. coli* in a soluble form. They are monodisperse, as judged by dynamic light scattering, and can be highly concentrated apart from p40^{phox}, which shows a tendency to aggregate at higher concentrations. Similar constructs have been shown in previous studies to retain their biological activity as judged by cell-free NADPH oxidase reconstitution assays, indicating that the proteins are correctly folded upon expression in *E. coli* (9, 12, 27, 33, 37). Prior to studying complex formation between the cytosolic *phox* components, we investigated potential self-association of the individual proteins in sedimentation equilibrium experiments. Analysis of these data can be used to derive the true molecular weight, without making any assumptions about the form and shape of the molecule(s) under investigation. Nine data sets at three different speeds and three concentrations were collected for each protein. Global fitting of these data sets to a single species resulted in a random distribution of residuals indicating that all three proteins exist as monomers in solution (Fig. 2*A*). The molecular masses determined for p40^{phox}, p47^{phox}, and p67^{phox} are 41,036, 43,892, and 61,621 Da, respectively, in good agreement with the formula molecular masses and those determined by electrospray mass spectrometry (39,966, 44,963, and 60,015 Da) (Table I). p67^{phox} has previously been described as forming dimers based on gel filtration chromatography and small angle neutron scattering studies (45). To investigate if this discrepancy with our data might be due to a non-globular shape of the protein, we carried out sedimentation velocity studies to derive an estimate for the asymmetry of p67^{phox} (Table II). The velocity data yielded a sedimentation coefficient ($s_{20,w} = 3.2 \times 10^{-13}$ s) and diffusion coefficient ($D_{20,w} = 4.7 \times 10^{-7}$ cm^2 s^{-1}), which are lower than would be expected for a globular protein of 60 kDa (Table II). The frictional ratio (f/f_0), which is an indication of the asymmetry of a protein, can be calculated from these data and has been found to be near 1.2 for globular proteins. The value calculated for p67^{phox}, however, is fairly high (f/f_0 = 1.65), indicating that the shape of p67^{phox} significantly deviates from that of a globular protein. Modeling these results as a prolate ellipsoid yields an axial ration a/b of 12.1, suggesting that p67^{phox} adopts an elongated shape in solution (Table II). This conclusion is further corroborated by dynamic light scattering studies that showed p67^{phox} to be monodisperse (polydispersity indices 0.1–0.2) and yielded a translational diffusion coefficient

TABLE I
Molecular masses determined from sedimentation equilibrium experiments

All measurements were carried out at three different loading concentrations and three different speeds as described under "Experimental Procedures" and fitted simultaneously. Standard deviations were calculated from fits to individual data sets. The theoretical molecular masses were calculated from the amino acid sequences, taking into account the amino acids that are left at the N terminus after cleavage with thrombin or PreScission protease. All listed values of M_{app} represent values obtained from fits of the data to ideal, single-component models.

Protein	Molecular mass	Theoretical molecular mass
	Da	
p67^{phox}	61,621 ± 2,800	60,015
p47^{phox}	43,892 ± 2,600	44,963
p40^{phox}	41,036 ± 3,700	39,966
p67^{phox}-p47^{phox}	105,160 ± 3,700	104,978
p67^{phox}-p40^{phox}	107,550 ± 10,000	99,981
p67^{phox}-p47^{phox}-p40^{phox}	144,546 ± 3,500	144,944
p47^{phox}-p40^{phox}	70,842 ± 2,500	84,929

TABLE II
Hydrodynamic shape parameters of p67^{phox} and the p40-p47-p67^{phox} complex

Conditions for sedimentation velocity and dynamic light scattering (DLS) measurements are described under "Experimental Procedures." $s^0_{20,w}$ and $d^0_{20,w}$ are the sedimentation coefficients and translational diffusion coefficients extrapolated to zero concentration and corrected to standard conditions. f/f_0 is the fractional ratio derived from $s^0_{20,w}$. *a/b* is the axial ratio calculated assuming a prolate ellipsoid model.

	p67^{phox}	p40-p47-p67^{phox}
$s^0_{20,w}$ (Svedbergs)	3.23	4.60
$d^0_{20,w}$ ($\times 10^{-7}$)cm^{2}s^{-1}	4.70	3.30
d^0(DLS) ($\times 10^{-7}$)cm^{2}s^{-1}	4.39	3.44
f/f_0	1.65	2.02
a/b	12.10	20.60

of 4.39 $\times$ 10^{-7} cm^2 s^{-1}, which was independent of the salt concentration from 50 to 500 mM NaCl. This value would be consistent with a molecular mass of 120 kDa in the case of a protein that holds a standard globular shape and hydration, close to that of a p67^{phox} dimer. Taken together, these hydrodynamic studies suggest that p67^{phox} adopts an extended and potentially flexible structure thus explaining its apparent dimeric behavior on gel filtration.

Formation of Dimeric Complexes between the Cytosolic Components of the NADPH Oxidase

The p40-p67^{phox} Complex—Isothermal titration calorimetry (ITC) allows direct measurement of the equilibrium binding constant K_a ($K_d = 1/K_a$) and the enthalpy of complex formation (ΔH) without the need for producing fusion proteins that can be attached to a solid surface, or the introduction of radioactive or spectroscopic labels. Titration of p40^{phox} into p67^{phox} was exothermic ($\Delta H = -5.4$ kcal/mol) and resulted in the formation of a very tight complex with a dissociation constant of 10 nM and a stoichiometry of 1:1 (Fig. 3*A* and Table III). This affinity is in reasonable agreement with that previously obtained by surface plasmon resonance studies (K_d = 43 nM (47)).

The p47-p67^{phox} Complex—The binding isotherm for the titration of p67^{phox} with p47^{phox} showed systematic deviations from a single-site binding model indicating that more than one binding event was taking place. Increasing the time between injections had no effect on this apparent biphasic behavior. A model assuming two independent binding sites resulted in a good fit and yielded dissociation constants of K_{d1} = 20 nM and K_{d2} = 150 nM and reaction enthalpies of $\Delta H_1 = -8.9$ kcal/mol and $\Delta H_2 = -4.6$ kcal/mol, respectively (Fig. 3*B* and Table III). Only the high affinity binding site was fully occupied whereas the second binding site exhibited a stoichiometry of 1:0.25 ($\pm$0.1). The occurrence of a second binding site was rather surprising especially considering the low occupancy of this site. To investigate if p67^{phox} might bind more than one molecule of p47^{phox} we carried out gel filtration analysis of complexes between p47^{phox} and p67^{phox} at varying stoichiometries. Fig. 4 shows that a 1:1 mixture elutes as a single species with a retention time that is shorter than that of the individual proteins. In contrast, mixtures containing a molar excess of p47^{phox} or p67^{phox} elute as two species where the second species corresponds to the excess protein (data not shown). Because the ITC data indicated that the second binding site is only between 15 and 30% occupied, we tested if an excess of as little as 10, 20, or 30% of p47^{phox} might be incorporated into a p47-p67^{phox} complex. As is shown in Fig. 4, even these small amounts resulted in the appearance of an additional p47^{phox} peak, clearly indicating that p47^{phox} and p67^{phox} exist in a stoichiometric 1:1 heterodimeric complex. This conclusion is further corroborated by sedimentation equilibrium studies of a 1:1 complex of p47-p67^{phox}. Fitting of these data to a single species model resulted in a good fit, with residuals that were randomly distributed about the zero value, indicating that the complex is a monodisperse species. The molecular mass calculated from this fit was 105,160 Da, which is in very good agreement with its theoretically calculated molecular mass of 104,978 Da (Fig. 2*B* and Table I). Taken together these observations suggest to us, that the second binding event that we have detected in the p47-p67^{phox} complex is not due to the binding of an additional molecule of p47^{phox} but must be an intrinsic feature of a stoichiometric p47-p67^{phox} complex (see "Discussion").

The p40-p47^{phox} Complex—p40^{phox} has been proposed to be the adaptor that links p47^{phox} to p67^{phox} in the cytoplasmic complex (41, 44, 45). However, titration of p40^{phox} with p47^{phox} did not result in any significant heat change suggesting that the two proteins either do not or only weakly interact, that the heat capacity of complex formation ΔC_p is such that ΔH is very small at the experimental temperature, and/or that the interaction is mainly entropy driven. To discriminate between these possible explanations, further studies were carried out using a variety of techniques. In surface plasmon resonance experiments using the BIAcore system, p40^{phox} was directly coupled to a Ni-NTA chip via its C-terminal hexahistidine tag, and binding of p47^{phox} was monitored. Although there was clear net binding of p47^{phox} to p40^{phox} the data were not of sufficient quality to be able to determine an equilibrium constant from kinetic "on" and "off" rates or equilibrium binding analysis (data not shown). This poor data quality is likely due to the fact that the interaction of the hexahistidine tag of p40^{phox} with the Ni-NTA chip does not seem to be sufficiently tight, resulting in the protein being partially washed off the chip during the experiment. Sedimentation equilibrium runs of a 1:1 mixture of p40^{phox} and p47^{phox} and fitting of the data to a single species model yielded a molecular mass of 70,842 Da providing further evidence that the two proteins interact in solution. However, analysis of these data assuming a monomer-dimer equilibrium is complicated by the fact that the two proteins have different extinction coefficients at 280 nm (ϵ = 39,400 M^{-1} cm^{-1} for p40^{phox} and ϵ = 57,750 M^{-1} cm^{-1} for p47^{phox}), which makes it impossible to correctly convert the association constant, which is calculated in absorbance units into molar concentrations. Nevertheless, because the molecular weights of the two proteins are very close and there is only a 1.4-fold difference in extinction coefficients, we assumed a mean value of ϵ_{280} = 48,575 M^{-1} cm^{-1} per monomer to estimate a lower limit of 4 μM for the dissociation constant. This value is in very good agreement with a previous estimation for the affinity of this complex, which has been made based on small angle neutron scattering studies (45).

Formation of the Trimeric p40-p47-p67^{phox} Complex

To investigate whether the occurrence of a two-site binding isotherm upon interaction of p67^{phox} with p47^{phox} is a particular feature of this complex or whether it also occurs if p67^{phox} is already complexed with p40^{phox}, we titrated a purified p40-p67^{phox} complex with p47^{phox}. Data from this titration could, again, only be fitted to a two-site binding model with dissociation constants of 14 and 128 nM and reaction enthalpies of -7.5 and -4.6 kcal/mol, respectively (Fig. 3*C*). As observed before, the second binding site exhibited a stoichiometry of 1:0.25 ($\pm$0.1). The similarity between results from this titration and that of p67^{phox} with p47^{phox} suggests that complex formation between p47^{phox} and p67^{phox} takes place independently of the presence of p40^{phox}. In addition, it confirms that p40^{phox} and p47^{phox} do not share a common binding site on p67^{phox}. As observed for the p47-p67^{phox} complex, a 1:1:1 mixture of p40^{phox}, p47^{phox}, and p67^{phox} elutes as a single species on gel filtration and addition of an excess of any of the components

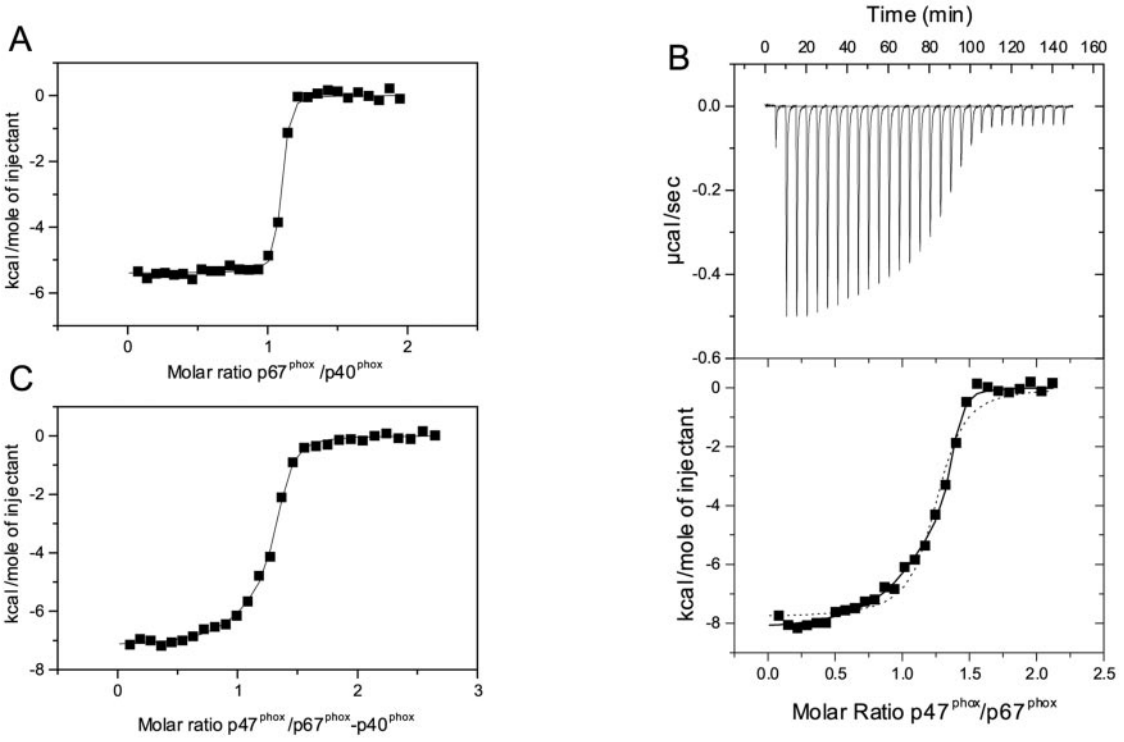

FIG. 3. **Isothermal titration calorimetry measurements of complex formation between *phox* proteins.** *A*, titration of 100 μM p67^{phox} into 11 μM p40^{phox}. The integrated heats from which the heat of dilution has been subtracted are shown as well as the fit to a single site binding isotherm that yielded K_d = 10 nM and $\Delta H = -5.4$ kcal mol^{-1}. Titration of *B*: 204 μM p47^{phox} into 21 μM p67^{phox} and *C*: 130 μM p47^{phox} into 13 μM p40-p67^{phox}. The raw data of the titration of p47^{phox} into p67^{phox} are shown in the *top panel* of *B*. The integrated heats from which the heat of dilution has been subtracted are shown in the other panels. Data shown in *B* and *C* could not be fitted to a single site binding model but had to be fitted to a two-site binding function. The *dotted line* in the *lower panel* in *B* shows a fit to a single site binding model, clearly indicating systematic deviations. Analysis of the data yielded: *B*, K_{d1} = 20 nM, $\Delta H_1 = -8.9$ kal/mol, n = 1.0 ± 0.15 and K_{d2} = 150 nM, $\Delta H_2 = -4.6$ kal/mol, n = 0.25 ± 0.1; *C*, K_{d1} = 14 nM, $\Delta H_1 = -7.5$ kcal/mol, n = 1.0 ± 0.1 and K_{d2} = 128 nM, $\Delta H_2 = -4.6$ kal/mol, n = 0.25 ± 0.1.

TABLE III

Thermodynamic parameters of complex formation between the cytosolic components of the NADPH oxidase

All measurements were performed in 25 mM HEPES, 50 mM NaCl, 1 mM EDTA, 2 mM dithiothreitol at pH 7.0, 7.5, or 8.0, depending on the pIs of the individual proteins and complexes formed. $T\Delta S$ was calculated from the measured values of K_a and ΔH. The stoichiometry of complex formation, N, is 1.0 ± 0.15 for titrations that were fitted to a single site binding model and N_1 = 1.0 ± 0.15 and N_2 = 0.25 ± 0.1 for titrations that had to be fitted to a two site binding model. The errors reflect standard deviations for repeated titrations.

Titration	K_{a1}	ΔH_1	$T\Delta S_1$	K_{a2}	ΔH_2
	$\times 10^7\ M^{-1}$	*kcal/mol*		$\times 10^7\ M^{-1}$	*kcal/mol*
p47^{phox} + p67^{phox}	5 ± 3	−8.9 ± 0.9	1.2	0.67 ± 0.2	−4.6 ± 1
p67-p40^{phox} + p47^{phox}	7.3 ± 1	−7.5 ± 0.3	2.8	0.78 ± 0.08	−4.6 ± 0.2
p47^{phox} (155-end) + p67^{phox}	8 ± 1	−9.8 ± 1.2	0.6	1.14 ± 0.5	−6.6 ± 1.1
p47^{phox} + p67^{phox} (234–end)	12.5 ± 3	−8.8 ± 0.4	1.9	1.1 ± 0.16	−4.8 ± 1.1
p47^{phox} + p67^{phox} (450–526)	4.8 ± 1.6	−7.4 ± 0.2	2.7		
p67^{phox} + p40^{phox}	10 ± 2.7	−5.4 ± 0.4	5.1		
p47^{phox} (1–295) + p67^{phox}	0.017 ± 0.006	−8.8 ± 0.9	−1.9		

results in the appearance of an additional peak (data not shown). Sedimentation equilibrium analysis of a 1:1:1 complex showed that it behaves as a single, monodisperse species with a molecular mass of 144,546 Da in good agreement with its formula molecular mass of 144,944 Da (Fig. 2*C*). DLS measurements of this complex confirmed its monodispersity (polydispersity index 0.3), however, a diffusion coefficient of 3.44 × 10^{-7} cm^2 s^{-1} determined by single-exponential cumulant analysis, which would be consistent with a molecular mass of 240 kDa in the case of a globular protein indicates that the shape of this complex deviates significantly from that of a globular protein. This observation is substantiated by sedimentation velocity studies from which a frictional ratio f/f_0 = 2.02 and an axial ratio a/b = 20.6 were calculated (Table II). These values are comparatively high for a protein but can be rationalized by the fact that all three components of this complex are multidomain proteins made up of individual domains that are connected by linkers that are likely to be rather flexible. This results in a heterotrimeric complex that adopts a highly elongated shape due to the asymmetry of one of its components (p67^{phox}) and due to its flexible organization.

Protein-Protein Interactions in the p47-p67^{phox} Complex

To further characterize the structural features of complex formation between p47^{phox} and p67^{phox} and to understand the reason for the occurrence of a biphasic binding isotherm, we have produced various N- and C-terminally truncated p47^{phox} and p67^{phox} fragments and assessed their behavior in ITC titrations in comparison to the full-length proteins.

The proline-rich region in the C terminus of p47^{phox} has invariably been suggested to be the target for the SH3 domain in p40^{phox} as well as C-terminal SH3 domain in p67^{phox}. To investigate if the tight, stoichiometric binding we detect in titrations of p67^{phox} with p47^{phox} is due to this interaction, we

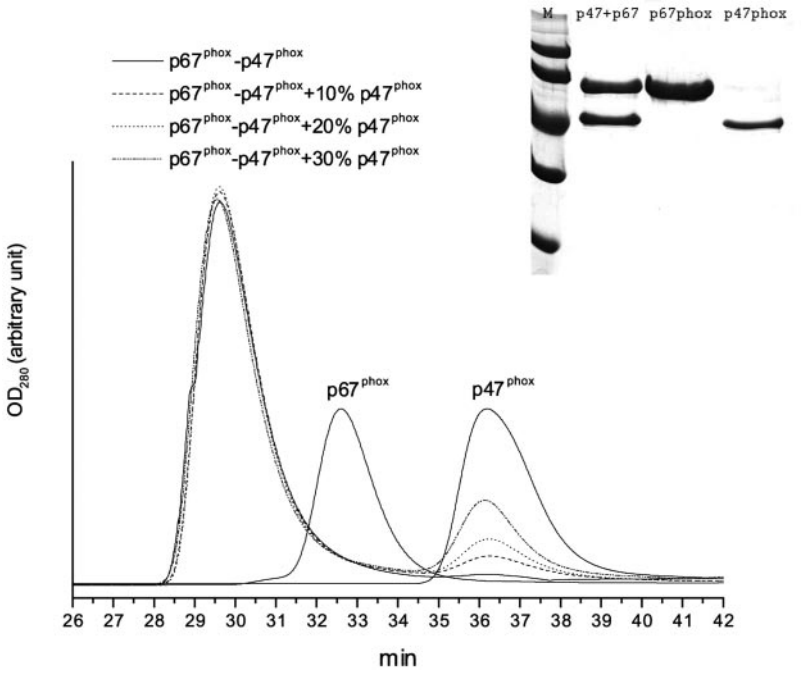

FIG. 4. **Analytical gel filtration of p47^{phox} and p67^{phox} and complexes thereof.** Gel filtration was performed in 50 mM Hepes, pH 7.0, 100 mM NaCl, and 2 mM $MgCl_2$ at a flow rate of 0.4 ml/min and protein concentrations of 50 μM. The *solid line* shows the elution profile of the individual p47^{phox} and p67^{phox} proteins as well as a 1:1 p47/p67^{phox} complex. The remaining lines show the elution profiles of a 1:1 mixture of p47^{phox} and p67^{phox} plus an excess of 10% p47^{phox} (*dashed line*), 20% p47^{phox} (*dotted line*), and 30% p47^{phox} (*dotted and dashed line*). *Inset*, fractions eluting at 29.5, 33, and 36.5 min were separated on a 12% SDS-polyacrylamide gel and stained with Coomassie Brilliant Blue.

measured complex formation between the isolated C-terminal SH3 domain of p67^{phox} and full-length p47^{phox} by ITC. This titration follows a single site binding isotherm with a 1:1 stoichiometry as would be expected for complex formation between an SH3 domain and its proline-rich target. Binding occurred with an affinity of 21 nM and a reaction enthalpy of −7.4 kcal/mol, indicating that this interaction indeed constitutes the high affinity binding site detected in titrations using the full-length proteins. This conclusion is further substantiated by the fact that removal of the proline-rich region (p47^{phox} 1–354) completely abrogated complex formation. Interestingly, further C-terminal truncation of p47^{phox} (fragment 1–295) to remove the polybasic region, which is thought to be responsible for the intramolecular masking of the tandem SH3 domains, restored binding and resulted in the formation of a 1:1 complex with a dissociation constant of 6 μM. This interaction results from a favorable enthalpy change, which is of similar size to that observed for the interaction between full-length p47^{phox} and p67^{phox}. However, in contrast to that interaction the entropy change exhibited here is unfavorable, resulting in a 300-fold lower affinity (Table III).

To investigate if the N-terminal region in p67^{phox}, including the TPR domain and the proline-rich region around amino acids 219–234 might contribute to the apparent biphasic behavior of p47-p67^{phox} complex formation, we deleted this region (p67^{phox} 234-end) and measured binding to full-length p47^{phox} by ITC. This construct behaved almost identically to full-length p67^{phox}. The titration had to be fitted to a two-site binding model and exhibited a tight, stoichiometric binding site with a K_d of 8 nM and ΔH of −8.8 kcal/mol, whereas the second binding event again showed an apparent stoichiometry of 1:0.25 (±0.1). Removal of the N-terminal portion of p47^{phox}, including the PX domain (p47^{phox} 155-end) had a similar effect, resulting in a two-site binding isotherm with a K_d of 12 nM and reaction enthalpy of −9.8 kcal/mol for the first site and a low stoichiometry occupancy for the second. The similarity of these titrations with those of full-length p47^{phox} and p67^{phox} but also p67-$SH3_B$ suggests to us that tight, stoichiometric complex formation between p67-$SH3_B$ and the proline-rich region of p47^{phox} occurs independently of the remainder of the two proteins and is not influenced by the second binding event detected in these titrations.

DISCUSSION

The NADPH oxidase is a multiprotein enzyme whose activity is regulated by the reversible formation of multiple protein-protein interactions between the cytosolic and membrane components as well as between the cytosolic proteins themselves. Many of these interactions involve SH3 domains and their target proline-rich sequences, which are present in p22^{phox}, p40^{phox}, p47^{phox}, and p67^{phox}. Activation of cells by appropriate stimuli leads to phosphorylation of p47^{phox}, which in turn induces intra- and intermolecular rearrangements within a number of these protein-protein interactions. This study was aimed at carrying out a detailed quantitative characterization of the protein-protein interactions, which occur in the resting state of the NADPH oxidase to establish a basis upon which the activation process can be investigated.

p40^{phox}, p47^{phox}, and p67^{phox} exist as a tight complex in the cytosol of resting neutrophils from which it can be purified by gel filtration with an apparent molecular mass of 250–300 kDa, twice that expected for a complex containing one copy of each of the proteins. Sedimentation equilibrium studies presented here show that the individual proteins exist as monomers, which associate to form a monodisperse, 1:1:1 complex. Addition of an excess of any of the individual proteins to this complex does not result in additional binding. The shape of this complex significantly deviates from that of a globular molecule as evidenced by dynamic light scattering as well as sedimentation velocity studies from which a fractional coefficient of 2.02 was derived. Thus the large molecular weight observed by gel filtration is not due to the existence of multiple copies of any of the proteins in this complex but is rather due to an extended shape and possibly flexible organization of the heterotrimer.

Extensive studies have been carried out to characterize the domains that mediate the protein-protein interactions within the p40-p47-p67^{phox} complex, but despite this wealth of data it is still unclear at which stage during the activation process a particular interaction occurs. Our data show that p40^{phox} and p67^{phox} form a very tight complex with a dissociation constant in the low nanomolar range. This interaction has been previously mapped to a region between the two SH3 domains in p67^{phox}, which contains the recently identified BP1 domain and its target sequence, the PC motif (phox and Cdc; also known as

the OPR motif)), which resides in the C-terminal part of p40^{phox} (50, 51). p40^{phox} has often been described as the primary binding partner for p47^{phox} in the resting state due to an interaction of its SH3 domain with the Pro-rich region in the C terminus of p47^{phox}. Consequently, many models for NADPH oxidase architecture assume that p40^{phox} is the link between p47^{phox} and p67^{phox}. However, this Pro-rich region in p47^{phox} has also been described to bind to p67^{phox} and possibly, in an intramolecular fashion, to its own tandem SH3 domains. Because a single, short proline-rich motif can only bind to a single SH3 domain at any one time, we carried out ITC studies to determine the affinities of the individual oxidase components for one another. We show that the affinity of p40^{phox} for p47^{phox} is comparatively low, in the micromolar range, in accordance with neutron scattering data, which estimated the affinity to be around 4.0 μM (45). In contrast, p47^{phox} binds to p67^{phox} with nanomolar affinity. To our surprise this titration did not follow a single site binding isotherm but could only be fitted assuming two non-identical sites. Despite this behavior, sedimentation equilibrium analyses and gel filtration chromatography of p47^{phox} and p67^{phox} at various ratios showed convincingly that p47^{phox} and p67^{phox} form a 1:1 complex. This clearly indicates that the second binding event detected by ITC does not reflect an additional binding site. Interestingly, binding of p47^{phox} to a preformed complex of p40-p67^{phox} exhibited a similar behavior. The agreement, within experimental error, between the K_d values and ΔH values for the stoichiometric binding site determined in these two experiments implies that the presence of p40^{phox} has no influence on complex formation between p47^{phox} and p67^{phox} in the resting state. By carrying out ITC titrations using a C-terminally truncated p47^{phox} as well as the isolated C-terminal SH3 domain of p67^{phox} we could show that the tight interaction that we detected between full-length p47^{phox} and p67^{phox} is due to binding of the C-terminal Pro-*X*-*X*-Pro motif in p47^{phox} to p67-SH3$_B$. Taken together, these results clearly demonstrate that p40^{phox} can not be the link between p47^{phox} and p67^{phox} in the resting state, because the affinity of p67^{phox} for the Pro-rich region in p47^{phox} is about 1000-fold higher than that of p40^{phox}.

Our ITC data for complex formation between full-length p47^{phox} and p67^{phox} indicated that a second process is taking place in addition to interaction of the two proteins via their respective C termini. This process has no influence on the C-terminal SH3 domain-proline-rich region interaction. ITC titrations using N-terminally truncated versions of either protein indicated that neither the PX domain of p47^{phox} nor the TPR domain of p67^{phox} is responsible for this process. At present we are not able to explain the reason for this second event and can only conclude that it seems to require the presence of the tandem SH3 domains of p47^{phox} that are masked by an intramolecular interaction with the subsequent polybasic region (24, 25) as well as the C-terminal half of p67^{phox}. Further studies are currently underway to explore this phenomenon.

Based on the data presented here combined with data from other reports we suggest the following model for the NADPH oxidase architecture in the resting state (Fig. 5). p67^{phox} is the bridge that connects p40^{phox} and p47^{phox}. No direct interaction takes place in this complex between p40^{phox} and p47^{phox}. Furthermore, association of p40^{phox} with p67^{phox} appears not to induce a conformational change in the p47^{phox} binding site of p67^{phox}, because binding of the latter to the C-terminal Pro-rich region of p47^{phox} follows a similar behavior in the absence or presence of p40^{phox}. p47^{phox} exists in an autoinhibited conformation in this complex in which its SH3 domains are masked by intramolecular interactions with a polybasic region in the C-terminal portion of the protein and possibly with the PX domain. Upon activation, phosphorylation induces a conformational change in p47^{phox}, which unmasks the tandem SH3 domains, thereby allowing binding to p22^{phox} and translocation to the membrane. Babior *et al.* (26) have shown that phosphorylation of Ser-359 or Ser-370 is absolutely required for translocation as well as oxidase activity. Interestingly, both of these serines are adjacent to the poly-proline motif, which is the target of the C-terminal SH3 domain of p67^{phox}, suggesting that phosphorylation might interfere with this interaction and may potentially induce the release of p67^{phox} rendering this sequence accessible for p40^{phox}. Our data show that a second binding site exists between p47^{phox} and p67^{phox} that is only accessible once the tandem SH3 domains of p47^{phox} have been unmasked. This site might become the primary interface between the two proteins if phosphorylation is capable of disrupting the "end-to-end" p47-p67^{phox} interaction. Further studies are now needed to describe in molecular detail the rearrangements that take place during the activation and assembly process.

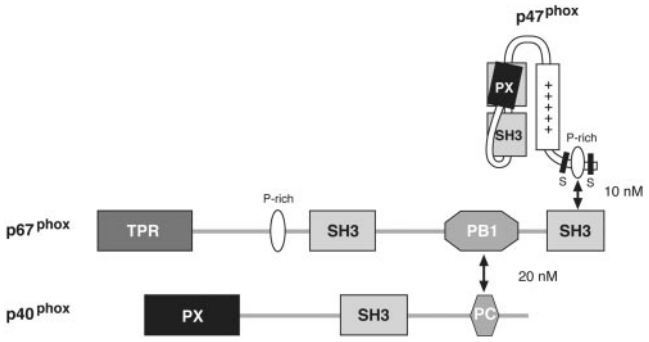

FIG. 5. **Model for the p40-p47-p67^{phox} complex in the resting state of the NADPH oxidase.** Domains are indicated by the same symbols as used in Fig. 1. p47^{phox} is shown in its autoinhibited form in which the polybasic region and possibly the PX domain interact with the tandem SH3 domains. The sites of protein-protein interactions are indicated by *arrows*. The positions of Ser-359 and Ser-370 in p47^{phox} are highlighted.

Acknowledgments—We thank Michael B. Yaffe (Massachusetts Institute of Technology, Harvard) for clones and plasmids and Frans Wientjes (University College London, London) for p40^{phox} in pET23. We are grateful to Steve Howell and Lesley Haire (National Institute for Medical Research) for mass spectrometry, John Eccleston for initial help with analytical ultracentrifugation, and Steve Smerdon, John Eccleston, and Ian Taylor for helpful discussions and critical reading of the manuscript.

REFERENCES

1. Babior, B. M. (1999) *Blood* **93,** 1464–1476
2. Clark, R. A. (1999) *J. Infect. Dis.* **179,** S309–S317
3. Nauseef, W. M. (1999) *Proc. Assoc. Am. Physicians* **111,** 373–382
4. McPhail, L. C. (1994) *J. Exp. Med.* **180,** 2011–2015
5. Park, J. W., Benna, J. E., Scott, K. E., Christensen, B. L., Chanock, S. J., and Babior, B. M. (1994) *Biochemistry* **33,** 2907–2911
6. Park, J. W., Ma, M., Ruedi, J. M., Smith, R. M., and Babior, B. M. (1992) *J. Biol. Chem.* **267,** 17327–17332
7. Wientjes, F. B., Hsuan, J. J., Totty, N. F., and Segal, A. W. (1993) *Biochem. J.* **296,** 557–561
8. Someya, A., Nagaoka, I., and Yamashita, T. (1993) *FEBS Lett.* **330,** 215–218
9. Shiose, A., and Sumimoto, H. (2000) *J. Biol. Chem.* **275,** 13793–13801
10. Huang, J., and Kleinberg, M. E. (1999) *J. Biol. Chem.* **274,** 19731–19737
11. Swain, S. D., Helgerson, S. L., Davis, A. R., Nelson, L. K., and Quinn, M. T. (1997) *J. Biol. Chem.* **272,** 29502–29510
12. Ago, T., Nunoi, H., Ito, T., and Sumimoto, H. (1999) *J. Biol. Chem.* **274,** 33644–33653
13. El Benna, J., Faust, R. P., Johnson, J. L., and Babior, B. M. (1996) *J. Biol. Chem.* **271,** 6374–6378
14. Park, J. W., and Babior, B. M. (1997) *Biochemistry* **36,** 7474–7480
15. Ellson, C. D., Gobert-Gosse, S., Anderson, K. E., Davidson, K., Erdjument-Bromage, H., Tempst, P., Thuring, J. W., Cooper, M. A., Lim, Z. Y., Holmes, A. B., Gaffney, P. R., Coadwell, J., Chilvers, E. R., Hawkins, P. T., and Stephens, L. R. (2001) *Nat. Cell Biol.* **3,** 679–682
16. Kanai, F., Liu, H., Field, S. J., Akbary, H., Matsuo, T., Brown, G. E., Cantley, L. C., and Yaffe, M. B. (2001) *Nat. Cell Biol.* **3,** 675–678
17. Cheever, M. L., Sato, T. K., de Beer, T., Kutateladze, T. G., Emr, S. D., and

Overduin, M. (2001) *Nat. Cell Biol.* **3,** 613–618
18. Xu, Y., Hortsman, H., Seet, L., Wong, S. H., and Hong, W. (2001) *Nat. Cell Biol.* **3,** 658–666
19. Ponting, C. P. (1996) *Protein Sci.* **5,** 2353–2357
20. Hiroaki, H., Ago, T., Ito, T., Sumimoto, H., and Kohda, D. (2001) *Nat. Struct. Biol.* **8,** 526–530
21. de Mendez, I., Homayounpour, N., and Leto, T. L. (1997) *Mol. Cell. Biol.* **17,** 2177–2185
22. de Mendez, I., Adams, A. G., Sokolic, R. A., Malech, H. L., and Leto, T. L. (1996) *EMBO J.* **15,** 1211–1220
23. Sumimoto, H., Hata, K., Mizuki, K., Ito, T., Kage, Y., Sakaki, Y., Fukumaki, Y., Nakamura, M., and Takeshige, K. (1996) *J. Biol. Chem.* **271,** 22152–22158
24. Sumimoto, H., Kage, Y., Nunoi, H., Sasaki, H., Nose, T., Fukumaki, Y., Ohno, M., Minakami, S., and Takeshige, K. (1994) *Proc. Natl. Acad. Sci. U. S. A.* **91,** 5345–5349
25. Leto, T. L., Adams, A. G., and de Mendez, I. (1994) *Proc. Natl. Acad. Sci. U. S. A.* **91,** 10650–10654
26. Johnson, J. L., Park, J. W., Benna, J. E., Faust, L. P., Inanami, O., and Babior, B. M. (1998) *J. Biol. Chem.* **273,** 35147–35152
27. Hata, K., Ito, T., Takeshige, K., and Sumimoto, H. (1998) *J. Biol. Chem.* **273,** 4232–4236
28. DeLeo, F. R., Nauseef, W. M., Jesaitis, A. J., Burritt, J. B., Clark, R. A., and Quinn, M. T. (1995) *J. Biol. Chem.* **270,** 26246–26251
29. Dusi, S., Donini, M., and Rossi, F. (1996) *Biochem. J.* **314,** 409–412
30. Heyworth, P. G., Curnutte, J. T., Nauseef, W. M., Volpp, B. D., Pearson, D. W., Rosen, H., and Clark, R. A. (1991) *J. Clin. Invest.* **87,** 352–356
31. Uhlinger, D. J., Tyagi, S. R., Inge, K. L., and Lambeth, J. D. (1993) *J. Biol. Chem.* **268,** 8624–8631
32. Diekmann, D., Abo, A., Johnston, C., Segal, A. W., and Hall, A. (1994) *Science* **265,** 531–533
33. Han, C. H., Freeman, J. L., Lee, T., Motalebi, S. A., and Lambeth, J. D. (1998) *J. Biol. Chem.* **273,** 16663–16668
34. Koga, H., Terasawa, H., Nunoi, H., Takeshige, K., Inagaki, F., and Sumimoto, H. (1999) *J. Biol. Chem.* **274,** 25051–25060
35. Koshkin, V., Lotan, O., and Pick, E. (1996) *J. Biol. Chem.* **271,** 30326–30329
36. Dang, P. M., Cross, A. R., and Babior, B. M. (2001) *Proc. Natl. Acad. Sci. U. S. A.* **98,** 3001–3005
37. Diebold, B. A., and Bokoch, G. M. (2001) *Nat. Immunol.* **2,** 211–215
38. Cross, A. R. (2000) *Biochem. J.* **349,** 113–117
39. Sathyamoorthy, M., de Mendez, I., Adams, A. G., and Leto, T. L. (1997) *J. Biol. Chem.* **272,** 9141–9146
40. Tsunawaki, S., Kagara, S., Yoshikawa, K., Yoshida, L. S., Kuratsuji, T., and Namiki, H. (1996) *J. Exp. Med.* **184,** 893–902
41. Fuchs, A., Dagher, M. C., Faure, J., and Vignais, P. V. (1996) *Biochim. Biophys. Acta* **1312,** 39–47
42. Finan, P., Shimizu, Y., Gout, I., Hsuan, J., Truong, O., Butcher, C., Bennett, P., Waterfield, M. D., and Kellie, S. (1994) *J. Biol. Chem.* **269,** 13752–13755
43. Ito, T., Nakamura, R., Sumimoto, H., Takeshige, K., and Sakaki, Y. (1996) *FEBS Lett.* **385,** 229–232
44. Wilson, L., Butcher, C., Finan, P., and Kellie, S. (1997) *Inflamm. Res.* **46,** 265–271
45. Grizot, S., Grandvaux, N., Fieschi, F., Faure, J., Massenet, C., Andrieu, J. P., Fuchs, A., Vignais, P. V., Timmins, P. A., Dagher, M. C., and Pebay-Peyroula, E. (2001) *Biochemistry* **40,** 3127–3133
46. Leusen, J. H., Verhoeven, A. J., and Roos, D. (1996) *J. Lab. Clin. Med.* **128,** 461–476
47. Wientjes, F. B., Panayotou, G., Reeves, E., and Segal, A. W. (1996) *Biochem. J.* **317,** 919–924
48. Philo, J. S. (1997) *Biophys. J.* **72,** 435–444
49. Wiseman, T., Williston, S., Brandts, J. F., and Lin, L. N. (1989) *Anal. Biochem.* **179,** 131–137
50. Ito, T., Matsui, Y., Ago, T., Ota, K., and Sumimoto, H. (2001) *EMBO J.* **20,** 3938–3946
51. Nakamura, R., Sumimoto, H., Mizuki, K., Hata, K., Ago, T., Kitajima, S., Takeshige, K., Sakaki, Y., and Ito, T. (1998) *Eur. J. Biochem.* **251,** 583–589